Intravenous Administration of Human Amniotic Mesenchymal Stem Cells in the Subacute Phase of Cerebral Infarction in a Mouse Model Ameliorates Neurological Disturbance by Suppressing Blood Brain Barrier Disruption and Apoptosis via Immunomodulation

Yasunori Yoshida[1], Toshinori Takagi[1], Yoji Kuramoto[1] ⓘ,
Kotaro Tatebayashi[1], Manabu Shirakawa[1], Kenichi Yamahara[2],
Nobutaka Doe[3,4], and Shinichi Yoshimura[1] ⓘ

Abstract

Neuro-inflammation plays a key role in the pathophysiology of brain infarction. Cell therapy offers a novel therapeutic option due to its effect on immunomodulatory effects. Amniotic stem cells, in particular, show promise owing to their low immunogenicity, tumorigenicity, and easy availability from amniotic membranes discarded following birth. We have successfully isolated and expanded human amniotic mesenchymal stem cells (hAMSCs). Herein, we evaluated the therapeutic effect of hAMSCs on neurological deficits after brain infarction as well as their immunomodulatory effects in a mouse model in order to understand their mechanisms of action. One day after permanent occlusion of the middle cerebral artery (MCAO), hAMSCs were intravenously administered. RT-qPCR for TNFα, iNOS, MMP2, and MMP9, immunofluorescence staining for iNOS and CD11b/c, and a TUNEL assay were performed 8 days following MCAO. An Evans Blue assay and behavioral tests were performed 2 days and several months following MCAO, respectively. The results suggest that the neurological deficits caused by cerebral infarction are improved in dose-dependent manner by the administration of hAMSCs. The mechanism appears to be through a reduction in disruption of the blood brain barrier and apoptosis in the peri-infarct region through the suppression of pro-inflammatory cytokines and the M2-to-M1 phenotype shift.

Keywords

cell therapy, amnion, ischemic stroke, MCAO, mouse, human amniotic mesenchymal stem cells

Background

Ischemic stroke is a major cause of permanent disability and death in people worldwide[1]. The neuro-inflammation that occurs following occlusion and deprivation of the blood supply plays an important role in the pathophysiology of ischemic stroke[2].

Lack of blood, due to a disruption of the blood supply, initiates ischemic damage through hypoxia, the production of reactive oxygen species, complement activation, alteration of blood brain barrier (BBB) permeability, and the increased expression of adhesion molecules, such as selectin and intracellular adhesion molecule-1 (ICAM-1),

[1] Department of Neurosurgery, Hyogo College of Medicine, 1-1 Mukogawa, Nishinomiya, Hyogo, Japan
[2] Laboratory of Medical Innovation, Institute for Advanced Medical Sciences, Hyogo College of Medicine, Nishinomiya, Hyogo, Japan
[3] Laboratory of Neurogenesis and CNS Repair, Hyogo College of Medicine, Nishinomiya, Hyogo, Japan
[4] Laboratory of Psychology, General Education Center, Hyogo University of Health Sciences, Kobe, Hyogo, Japan

Corresponding Author:
Shinichi Yoshimura, Department of Neurosurgery, Hyogo College of Medicine, 1 -1 Mukogawa, Nishinomiya, Hyogo, Japan.
Email: hyogoneuro@yahoo.co.jp

on capillary vessels[2–5]. This is followed by the adhesion and infiltration of neutrophils and circulating monocytes. These blood-borne immune cells and perivascular macrophages release neurotoxic mediators such as matrix metalloproteinase9 (MMP9), tumor necrotic factor α (TNFα), nitric oxide (NO), and interleukin 1β (IL1β), leading to further BBB breakdown and enhanced leukocyte infiltration[2,6–9]. Neuronal cell death causes the next phase of the inflammatory response, resulting in the release of damage-associated molecular pattern proteins, which activate parenchymal macrophages and microglia resulting in the production of pro-inflammatory cytokines such as interleukin23 (IL23), IL1β, and TNFα[2,7]. This is followed by the induction of IL23 induced interleukin-17-producing γδ T lymphocytes, which then act on macrophages to promote neurotoxic effects[2,7]. Although this process promotes clearance of dead tissue and neuro-regeneration, excessive inflammation often interferes with tissue repair and exacerbates the damage caused by the primary injury[2,7,10].

Currently, intravenous administration of the recombinant tissue plasminogen activator and endovascular thrombectomy are performed worldwide as standard reperfusion therapies in the hyperacute phase for normalizing blood supply to ischemic penumbra, and for minimizing the ischemic core. However, these therapies are characterized by narrow time windows, and good outcomes are achieved only in a limited number of patients, even when these therapies are successfully performed. Furthermore, anti-inflammatory agents that block a single molecular pathway, such as ICAM1, the IL1 receptor, or neutrophils, have been studied as potential novel therapeutics in the management of cerebral infarction, although most of these studies failed[11,12]. Therefore, there is a need to focus on novel innovative therapeutic options.

Cell therapy has recently been recognized as an innovative therapeutic option for various neurological disorders[13]. It can target both the subacute and chronic phases of cerebral infarction, thereby providing an opportunity to manage chronic symptoms[14]. Stem cells used for treating ischemic infarction may be obtained from several sources, such as human embryonic stem cells (ES cells), induced pluripotent cells, and mesenchymal stem cells (MSCs)[13,14]. Among these, MSCs exhibit a unique feature, wherein these cells can exert their biological effects on neurogenesis, angiogenesis, cytokine production, and immunomodulation[14–18].

Amniotic stem cells, which are multipotent stem cells possessing phenotypic features similar to those of bone marrow-derived mesenchymal stem cells[10,19], modulate immune responses by suppressing the production of excessive pro-inflammatory cytokines and enhancing the production of anti-inflammatory cytokines. Thus, full advantage of these immunomodulatory effects may be taken by administering amniotic stem cells during the early stages of stroke, thereby promoting the beneficial effects of inflammation during the early stages, while regulating its harmful effects later on[10,20].

Furthermore, amniotic stem cells are unique in their immune tolerance, which is consistent with the functions of the amnion to protect the fetus from the mother's immune system[10,20,21]. Host responses have not been reported following xenotransplantation into immunocompetent animals, and this feature confers a unique advantage to amniotic stem cells, with particular reference to allogeneic therapeutic applications without immunosuppressants[19].

We have successfully isolated, expanded, and formulated human amnion derived mesenchymal stem cells (hAMSCs), derived from human fetal membranes[22], and demonstrated their immunomodulatory effects including the suppression of macrophage[23] and Th1/Th17 immunity[24]. For use as a potential drug, validation of the safety and efficacy of administering hAMSCs intravenously to patients with treatment resistant Crohn's disease and acute graft-versus-host disease is now under investigation with respect to their immunomodulatory effects via phase I/II clinical trials[25,26].

The objective of this study was to evaluate the therapeutic effects of hAMSCs on neurological deficits in a mouse model of cerebral infarction. Furthermore, we investigated the mechanisms underlying the immunomodulatory effects of these cells.

Materials and Methods

Animals

The study protocol was approved by the Animal Care Committee of Hyogo College of Medicine (Approval number: 17-034) and performed in accordance with the 'Guide for the Care and Use of Laboratory Animals' published by the National Academy of Science of the USA. Seven to nine-week-old male CB-17/Icr-+/+Jcl mice (Clea Japan Inc., Tokyo, Japan) were housed in a temperature (22-24°C) and humidity (55%) controlled room under a 12/12 light–dark schedule. The animals were allowed access to water and standard pellet chow ad libitum.

Induction of Permanent Focal Cerebral Infarction by Direct Occlusion of the Middle Cerebral Artery (MCAO) in Mice

The procedure was performed according to a previously described method[27]. Prior to surgery, the mice were anesthetized using 2% isoflurane. Briefly, an incision was made in the skin between the left eyeball and the left ear hole. The left zygoma was dissected and detached under an operating microscope. A bone window (diameter: 1.5 mm) was made using a dental drill, and the main trunk of middle cerebral artery (MCA) was electrocauterized and cut down just distal to the olfactory tract to induce a permanent focal cerebral infarction (Mylan, Canonsburg, Pennsylvania, USA). This method has been reported to confer a number of advantages when investigating the therapeutic effects of experimental treatments on ischemic infarction. These advantages are as

follows: (a) the model produces highly reproducible lesions of cortical infarction; (b) mice show long-term survival; and (c) it is a model of permanent focal ischemia which mimics the pathophysiology of actual human cerebral infarctions. A sham surgery was also performed in control mice. For sham surgery, all the arteries were exposed for the surgical period, but the MCA was not occluded.

Cell Preparation and Administration of hAMSCs

The hAMSCs were prepared as previously described[22]. Briefly, informed consent was obtained from all donors who provided fetal membranes according to the protocol approved by our institutional ethic committee (approval number 325). The fetal membranes were obtained from healthy donor mothers following a cesarean section. The amnion was mechanically separated from the chorion and processed with collagenase/dispase solution. Following this, the cells were suspended in minimal essential medium with bovine-derived platelet lysate "NeoSERA®" (https://www.japan-biomedical.jp) and incubated at 37°C for cell expansion. Mice were randomly assigned to four groups as follows: high-dose hAMSC group (MCAO followed by administration with a high dose of hAMSCs); low-dose hAMSC group (MCAO followed by administration with a low dose of hAMSCs); the vehicle control group (MCAO followed by administration of lactated Ringer's solution alone); and sham group (administration of lactated Ringer's solution after sham surgery). Mice in the first and second groups received an intravenous injection of either 100 μL or 50 μL of hAMSCs (4×10^6 and 2×10^6 cells/kg) via the carotid vein under direct view 24 h after MCAO the induction of MCAO, respectively. Mice in the third and fourth groups received an intravenous injection of lactated Ringer's solution alone.

Behavioral Tasks

During the period between 1 and 2 months post-MCAO, a series of behavioral tasks were conducted on mice who had undergone MCAO, including the open field test, the wire hang test, the Y-maze task, the water maze learning task, the passive avoidance learning task, and the open space swimming test. These tasks were conducted to assess the functional deficits and recovery of the animals. Assessments were conducted by independent experimenters who were blinded to the experimental groups. Increase in general activity and anxiety after ischemic infarction[28,29] and the degree of impairment in habituation after repeated exposure, which reflects memory disturbance[30], were measured as locomotion counts by the open field test. Motor coordination and muscular strength were tested with the help of a wire hang test. Cognitive functions were assessed by the Y-maze, water maze learning, and passive avoidance learning tasks. Finally depression-like symptoms were also assessed using

the open space swimming test[31]. Details of the methods used are described in the supplemental material.

Quantitative Real-Time RT–PCR (q-PCR)

Seven days post-MCAO, mice in three groups (i.e., the high-dose hAMSC group, vehicle control group, and sham surgery group) were euthanized using isoflurane and decapitated. Ipsilateral hemispheres of the brain samples were quickly isolated and incubated in RNAlater RNA Stabilization Reagent (Qiagen, Hilden, Germany). Total RNA was extracted using a RNeasy mini kit (Qiagen) according to the manufacturer's instructions. The purified total RNA was converted into cDNA using ReverTra Ace qPCR RT Master Mix (Toyobo, Osaka, Japan), following which real-time PCR was performed using THUNDERBIRD SYBR qPCR Mix (Toyobo) according to the manufacturer's instructions. The relative expression levels of the housekeeping genes glyceraldehyde 3-phosphate dehydrogenase (GAPDH) as well as TNFα, MMP2, MMP9, and inducible nitric oxide synthase (iNOS) were determined. The primer sequences used for real-time PCR are listed [Additional file 1]. The levels of target gene expression were calculated via the ΔΔCT method and normalized against those of GAPDH.

Immunohistochemistry

Seven days post-MCAO, mice in two groups (i.e., the high-dose hAMSC group, and vehicle control group) were euthanized using isoflurane and decapitated. Brain tissues were fixed overnight in 4% paraformaldehyde, dehydrated in 30% sucrose, frozen at –80°C, and sliced into 10 μm coronal sections using a cryostat. Frozen sections were placed in PBS and a blocking solution (0.3% H_2O_2 in methanol) consecutively for 10 min each. They were then washed with PBS thrice for 3 min each time and placed in a permeabilization solution for 10 min (1% TritonX-100 in PBS). They were washed again with PBS twice for 5 min each time and placed in the blocking solution for 30 min at 25°C (0.1 M TBS containing 20% bovine serum and 3% BSA). The sections were then incubated overnight at 4°C with an anti stem101 antibody (1:100; Takara, Shiga, Japan, Y-40400), Diaminobenzidine (DAB) was used as a chromogen, and the nuclei were counterstained with hematoxylin. In fluorescent immunohistochemistry, non-specific binding was blocked with Blocking One Histo (Nacalai Tesque, Kyoto, Japan) according to the manufacturer's instructions, and permeabilized with 1% Triton X-100 in PBS for 10 min. The sections were incubated overnight at 4°C with an anti-iNOS antibody (1:500; Funakoshi, Tokyo, Japan, MAB9502), or an anti-CD11b/c antibody (1:100; Bioss, Woburn, USA, bs-1014R), and then incubated with corresponding Alexa Fluor 488- or 555-conjugated secondary antibodies (Cell Signaling Technologies, Danvers, Massachusetts, USA) at room temperature for 2 h. Nuclei were counterstained with 4′,6-diamino-2-phenylindole (DAPI; Sera Care, Milford,

Iowa, USA). Histological images were captured using a fluorescence microscope BZ-X (Keyence Corporation, Osaka, Japan) at a magnification of 200 x in order to count iNOS or CD11b/c positive cells. Eighteen fields in each of the peri-infarct areas (three non-overlapping random visual fields per coronal section and two sections per brain; $n = 3$ in each group) from both the high-dose hAMSC group and the vehicle control were analyzed by automatic cell counting, which was conducted using the hybrid cell count software BZ-X analyzer (Keyence Corporation). Luminance and separation of captured images were adjusted and cells were differentiated from debris based on their area and circularity. The images were then automatically batch counted. Contrarily, DAB-stained cells labeled as stem101-positive were manually counted using a light microscope (Keyence Corporation). The sample size and method used for image capture were in accordance with the immunofluorescence staining requirements.

The ischemic core was observed as a clearly demarcated necrotic area with low cell density and rich in debris and the peri-infarct area was observed as an area with a high degree of cell accumulation surrounding an ischemic core (Fig. 2a)[32,33].

Western Blotting

Seven days post-MCAO, mice in three groups (i.e., the high-dose hAMSC group, vehicle control group, and sham surgery group) were euthanized using isoflurane and decapitated. Ipsilateral hemispheres of the brain samples taken from all the groups were quickly frozen at $-80°C$, homogenized, and lysed using an EzRIPA Lysis kit according to the manufacturer's instructions (Atto Corporation, Tokyo, Japan). Protein levels in the whole lysates were measured using a BCA assay (Thermo Scientific, Waltham, Massachusetts, USA), and 20 µg of each protein sample was separated by 10% SDS-PAGE and then electrophoretically transferred to a PVDF membrane (Atto Corporation). Membranes were blocked in EzBlock Chemi (Atto Corporation) and probed with each antibody overnight. The membranes were then incubated with appropriate horseradish peroxidase-conjugated secondary antibodies after washing with 1% Triton X-100 in Tris buffered saline (TBS). Immunoreactive proteins were detected using an enhanced chemiluminescence kit (EzWestLumi plus, Atto Corporation) and visualized using LuminoGraph 1 (Atto Corporation). Quantification of immunoreactive proteins was performed using Image J software (NIH, Bethesda, MD, USA). The following antibodies were used in these experiments: anti-TNFα (1:200, Santa Cruz, Dallas, TX, USA, sc-52746), and anti-caspase3 (1:200, Santa Cruz, CA, USA, sc-7272).

Gelatine Zymography

The protein extracts were prepared and normalized using the process described for western blotting. Gelatine zymography
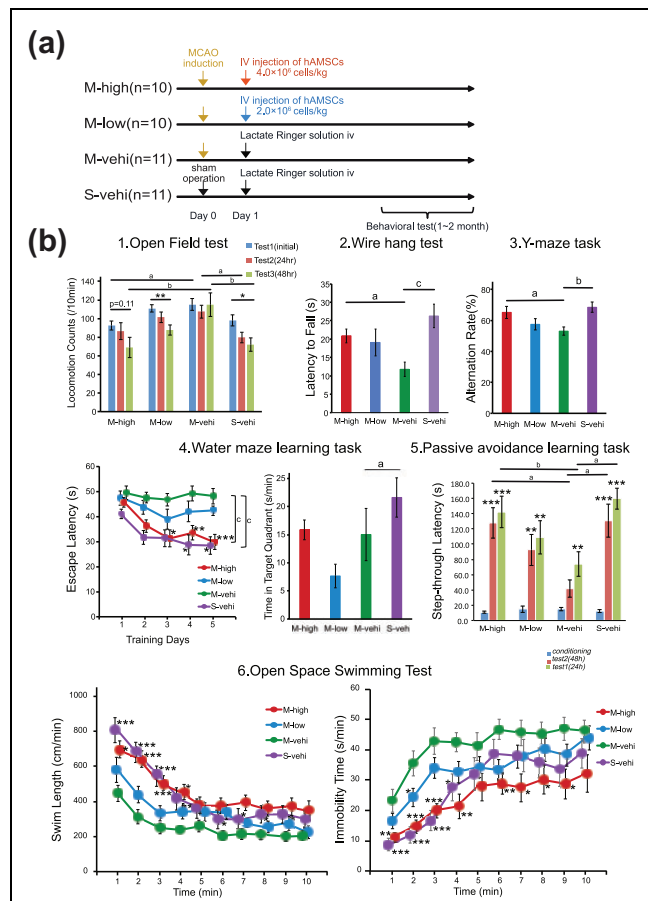

Figure 1. Acute intravenous administration of hAMSCs improves functional recovery following permanent MCAO. (a) Protocol for the evaluation of behavioral tasks. Behavioral testing was conducted using CB17 male mice randomly assigned to one of four arms: M-high (MCAO followed by the intravenous administration of a high dose of hAMSCs at 24 h; $n = 10$), M-low (MCAO followed by the intravenous administration of a low dose of hAMSCs at 24 h; $n = 10$), M-vehi (MCAO followed by the administration of vehicle alone; $n = 11$), and S-vehi (administration of vehicle following sham surgery; $n = 11$). The dose of hAMSCs was 4.0×10^6 cells per kg in the M-high group, and 2.0×10^6 cells per kg in the M-low group. Behavioral testing was conducted between 1 and 2 months post-MCAO. (b) The open field test, the wire hang test, the Y-maze task, the water maze learning task, the passive avoidance task, and the open space swimming test were conducted. [a] $P < .05$, [b] $P < .01$, [c] $P < .001$, Dunnett's test for the between-subject differences. *$P < .05$, **$P < .01$, ***$P < .001$, Dunnett's test for the between-subject differences in the open space swimming test and repeatedly measures within-subject differences for other behavioral tasks. For repeatedly measured data, a two-way repeated measures ANOVA was conducted first while for comparisons among more than three groups, one-way ANOVA was conducted first. Significant main effects of group and group by time interaction effects were suggested, except for an interaction effect for locomotion counts in the open field test, F (5, 62) = 0.817, P = .267.

was performed to measure MMP gelatinase activities according to the manufacturer's instructions (Cosmo Bio Corporation, Tokyo, Japan). The samples were subjected to electrophoresis in the precast gels. Following this, the gels

were incubated in renaturing buffer to remove SDS for 1 h, incubated in developing buffer at 37°C for 48 h, and then stained with Coomassie Blue for 30 min. Finally, the gels were decolorized and scanned using the white light image scanner ES-8500 (Epson, Suwa, Japan).

Evans Blue Assay

BBB permeability was assessed in mice from two groups (i.e., the high-dose hAMSC group, and vehicle control group) via the extravasation of Evans blue (EB), an index of albumin leakage. As previously described[34], Evans blue dye (4% in PBS, 4 mL/kg) was administered via the carotid vein 48 h following MCAO, which was 24 h after the administration of hAMSCs. Mice were euthanized and transcardially perfused with 100 mL of saline 2 h after EB dye administration at room temperature to wash out intravascular EB. Next, whole brains were quickly obtained. The ipsilateral hemisphere, contralateral hemisphere, and cerebellum, from each whole brain were separated from each other, and weighed. The samples were incubated in formamide (0.5 mL) at 55°C for 2 days. Supernatants were separated via centrifugation (15,000 × g, 10 min) following which the EB levels in supernatants were estimated, by measuring corresponding fluorescence at a wavelength of 620 nm, using a spectrophotometer (SPECTRA max PLUS384, Molecular Devices, San Jose, CA, USA). Tissues were then oven dried at 95°C for 5 days to obtain their dry weight. The EB levels in the brain samples was quantified using a standard linear regression curve using 11 concentrations (0–104 ng/mL) of EB dye and levels expressed as μg/brain. Relative EB levels were expressed as fold change of the contralateral side, corrected with brain dry weight.

Terminal Deoxynucleotidyl Transferase (TdT)-Mediated dUTP Nick End Labelling (TUNEL) Assay

In order to detect apoptotic cells, a TUNEL assay was performed in the mice from two groups (i.e., the high-dose hAMSC group, and the vehicle control group) according to the manufacturer's instructions (In situ cell death detection kit, POD; Sigma-Aldrich, St. Louis, Missouri, USA). Briefly, brain tissues were fixed overnight with 4% paraformaldehyde and cryoprotected in 30% sucrose. Frozen sections were placed in PBS for 30 min, blocking solution for 10 min (3% H_2O_2 in methanol), PBS for 10 min, permeabilization solution for 2 min on ice (0.1% TritonX-100 in 0.1% sodium citrate), washed three times with PBS for 3 min each time, placed in blocking solution for 30 min at room temperature (0.1 M TBS containing 20% bovine serum and 3% BSA), and then washed three times with PBS for 3 min each time. DNA strand breaks were labeled using fluorescein-12-dUTP by incubating with TdT buffer for 60 min at 37°C. As a negative control, the incubation was performed without the TdT enzyme. DAB was used as a chromogen, and the nuclei were counterstained with hematoxylin.

Neurons showing chromatin condensation, nuclear budding and fragmentation, or apoptotic bodies were identified as being apoptotic, whereas cells showing diffuse cytoplasmic labeling were considered as necrotic cells. Cells labelled as positive were manually counted using a light microscope (Keyence Corporation) at 400× magnification. The sample size and method for image capture were in accordance with immunofluorescence staining requirements.

Statistical Analysis

All data were expressed as mean ± SEM. JMP ver. 13 (SAS Institute Inc., Cary, NC, USA) was used to analyze data. Differences between two groups (i.e., the high-dose hAMSC group versus the vehicle control group) were analyzed for statistical significance via an unpaired two-tailed t-test, whereas differences between more than three groups were assessed using the post-hoc Dunnett's test if the one-way analysis of variance (ANOVA) was significant. For data obtained using repeated measurements (i.e., the open field test, escape latency of the water maze learning task, the passive avoidance learning task, and the open space swimming test), a two-way repeated measures ANOVA was first conducted to compare groups (i.e., the high-dose hAMSC group, the low-dose hAMSC group, the vehicle control group, and the sham surgery group) as the between-subject factor and repeated measures (sessions or days) as the within-subject factor. Only after these statistical analyses turned out to have significant main effects of group or the group by time interaction effects, we performed a Dunnett's test. When performing the Dunnett's test, the vehicle control group and initial sessions were set as the control for the comparisons between groups and for the analysis of within-subject differences, respectively. Statistical significance was set at $P < .05$.

Results

Acute Intravenous Administration of hAMSCs Improves the Neurological Deficits Induced by Cerebral Infarction in a Mouse Model of MCAO

On the day following the MCAO operation hAMSCs were administered intravenously and their therapeutic effects were then evaluated during the chronic phase of the disease (Fig. 1a). Mice who underwent the MCAO operation ($n = 31$) were randomly assigned to experimental groups as follows: the high-dose hAMSC group (M-high; $n = 10$); the low-dose hAMSC group (M-low; $n = 10$); and the vehicle control group (M-vehi; $n = 11$). We also performed sham surgery for the sham surgery group (S-vehi; $n = 11$); (Fig. 1a).

For data arising from repeated measures (i.e., the open field test, escape latency of the water maze learning task, the passive avoidance learning task, and the open space swimming test), there were significant main effects of group and

group by time interaction effects, except for an interaction effect for locomotion counts in the open field test, F (5, 62) = 0.817, P = .267.

Compared with mice in the S-vehi group, mice in the M-vehi group exhibited significant behavioral abnormalities in several behavioral tasks. In the open field test, across-session habituation decreases, which reflect a time-dependent decline in locomotion counts, were significantly more evident in the M-vehi group than in the S-vehi group (*P < .05) (Fig. 1b-1). This resulted in a clear trend in more apparent trend of hyperactivity and anxiety in the M-vehi group than in the S-vehi group in all the sessions ([a] P < .05, [b] P < .01) (Fig. 1b-1). These data suggest that MCAO mice develop general hyperactivity and an impairment in habituation reflecting memory disturbance. In the wire hang test, the latency to fall was significantly shorter in the M-vehi group than in the S-vehi group ([c] P < .001) (Fig. 1b-2), suggesting that MCAO mice have muscular weakness and a motor coordination deficit. In the Y-maze task, the percentage of alternation behaviors significantly decreased in the M-vehi group compared with that in the S-vehi group ([b] P < .01);(Fig. 1b-3). This result indicates that MCAO mice developed an impairment in their working memory. In the acquisition training sessions in the water maze learning task, mice in S-vehi group showed a clear decrease in escape latency (*P < .05, [c]P < .001) (Fig. 1b-4). This was not the case for mice in M-vehi group, who took a longer time to reach the hidden platform throughout the 5 days of training. In the probe test trial, mice in the M-vehi group stayed significantly less time (nearly chance levels) in the target quadrant than mice in the S-vehi group after excluding an outliner in the M-vehi group ([a] P < .05) (Fig. 1b-4). These results suggest that spatial learning and memory in the MCAO mice are impaired and that mice in the M-vehi group spent most of their time "floating" throughout this task[35]. In the passive avoidance learning task, there was no significant difference between the M-vehi and S-vehi groups in the step-through latency in the baseline conditioning trial. Because mice received an electric shock, the step-through latency was prolonged in both the M-vehi and S-vehi groups, indicating that both types of mice acquired avoidance behavior (**P < .01, ***P < .001) (Fig. 1b-5). Mice in the M-vehi group, however, showed a shorter step-through latency in the test trials than mice in the S-vehi group ([b]P < .01) (Fig. 1b-5). These results suggest that MCAO mice have a memory impairment. The open space swimming test showed that mice in the S-vehi group had longer swim lengths and a shorter immobility time compared with mice in the M-vehi group, indicating the development of depression like symptoms in MCAO mice, which is also consistent with the result of mostly "floating" M-vehi mice in the water maze learning task (*P < .05, **P < 0.01, ***P < 0.001) (Fig. 1b-6).

To evaluate the effect of administration of hAMSCs on general activities, motor function deficits, cognitive impairment, and depression-like symptoms in MCAO mice, we compared performance on the behavioral tests between MCAO mice who had administered hAMSCs (M-high and M-low groups) and the vehicle control (M-vehi). The open field test showed significant between-group differences for the M-high and M-vehi group in the sessions performed on day 1 and 3 ([a]P < .05, [b]P < .01) (Fig. 1b-1). The time-dependent decline in locomotion counts in the M-high group was not significant (P = .11), but there was an apparent trend for a decrease in locomotion counts in the M-high group compared with the M-vehi group (Fig. 1b-1). These findings indicate that there is recovery of habituation and a suppression of hyperactivity following administration of a high-dose of hAMSCs. The wire hang test demonstrated that there was a significant elongation of latency to fall in the M-high group compared with the M-vehi group, indicating that there is a recovery of motor function following administration of a high-dose of hAMSCs ([a]P < .05) (Fig. 1b-2). In addition, the Y-maze task showed that the alteration rate in the M-high group was significantly better than in the M-vehi groups, suggesting that there was a recovery in working memory in mice in the M-high group ([a]P < .05) (Fig. 1b-3). The water maze learning task also revealed that there was a significant decrease in escape latency in the M-high group unlike in the M-vehi group, suggesting that the partial recovery of learning and memory facilitated mice in M-high to explore and escape to a platform unlike the "floating" mice in the M-vehi group (*P < .05, **P < .01, *** P < .001, [c]P < .001) (Fig. 1b-4). There were no differences among the M-high, M-low, and M-vehi groups in the probe test trial. However this might be because the incomplete spatial learning and memory in the M-high group could not facilitate their straightforward escape but instead used random exploration along the wall (i.e., thigmotaxia[35]), which reduces the staying time in the target quadrant to nearly chance levels in the absence of a platform. The difference in the range of the standard error between M-vehi and M-high groups also suggests that mice in rhe M-vehi group were floating whereas mice in the M-high group were exploring with thigmotaxia. Furthermore, the passive avoidance learning task showed that the step-through latency in the M-high group was significantly better than that in the M-vehi group ([a]P < .05, bP < .01) (Fig. 1b-5). On the other hand, the open space swimming test revealed that mice in the M-high group swam longer than those in the M-vehi group whereas mice in the former group stopped swimming shorter than those in the latter group (*P < .05, **P < .01, ***P < .001) (Fig. 1b-6). The differences between these two groups were diminished as time passed due to subject fatigue. These data suggest that the depression-like symptoms seen after ischemic infarction were ameliorated by the administration of a high-dose of hAMSCs. Finally, all results from the behavioral tasks in the M-low group were better than that in the M-vehi group, indicating a tendency toward improvement compared with the M-vehi group, although this improvement was not statistically significant (Fig. 1b).

Taken together, these results indicate (i) that previously mentioned neurological and behavioral impairments, such as

general activities, motor weakness, memory impairment, and depression-like symptoms, in the mouse model of MCAO were indeed induced by cerebral infarction, and (ii) that these deficits were improved by administering hAMSCs in a dose dependent manner 2 to 3 months after MCAO.

The Administration of hAMSCs Suppresses mRNA Expression and Protein Expression Levels of Pro-Inflammatory Cytokines Around the Infarcted Brain During the Early Phase of Ischemic Infarction

The significant differences in the scores in the behavioral tasks between the M-high and M-vehi groups led us to assess the underlying mechanisms of the amelioration of symptoms after the administration of hAMSCs. The mRNA expression levels of pro-inflammatory cytokines in the brain were assessed 7 days after the induction of MCAO (Fig. 2a).

The relative mRNA expression levels of iNOS, MMP2, MMP9, and TNFα were significantly higher in the M-vehi group compared with the S-vehi group ($P < .01$), while these expression levels were significantly suppressed in the M-high group ($P < .01$) (Fig. 2a). A similar trend was also observed in the western blotting results for TNFα, although the difference was not statistically significant ($P = .088$) (Fig. 2b). Additionally, we performed gelatin zymography to evaluate matrix metalloproteinase activity in brain lysates. The MMP9 activity in the S-vehi group was close to zero (Fig. 2c) and was significantly lower in the M-high group compared with that in the M-vehi group ($P < .05$), although the MMP2 activity remained unchanged between these two groups (Fig. 2c).

These data suggest that administering hAMSCs suppresses the mRNA expression levels and the amount of pro-inflammatory cytokines around the infarcted brain in the early phase of ischemic infarction.

After the Intravenous Administration of hAMSCs, Stem101-Positive Cells Were Detected and the Infiltration of iNOS-Positive Pro-Inflammatory Immune Cells Was Suppressed in the Peri-Infarct Area.

To investigate whether intravenously administered hAMSCs migrated into the brain parenchyma and to analyze the distribution of immune cells showing pro-inflammatory neurotoxic phenotypes in the peri-infarct area, frozen brain sections of mice in the M-high and M-vehi groups were assessed via immunohistochemistry 7 days after MCAO. In the frozen brain sections DAB-stained with the anti-stem101 antibody, which specifically reacted with the human nucleus protein Ku80 and can differentiate implanted human cells from mouse brain tissues, we identified stem101-positive cells around the peri-infarct area in M-high mice (Supplemental Fig. S1). Although it was difficult to verify the absence of stem101-positive cells in the

M-vehi group due to the non-specific DAB staining characteristic of the ischemic core, stem101-positive cell counts around the peri-infarct area in the M-high group were significantly higher than those in the M-vehi group, which suggested that grafted stem101-positive hAMSCs migrated and survived in the the peri-infarct area of the mouse model at least 6 days after administration.

Fluorescent immunohistochemistry of CD11b/c showed an accumulation of CD11b/c positive immune cells in the peri-infarct area, suggesting the activation of macrophages and microglia. The distribution of iNOS-positive cells showed the same trend as the distribution of CD11b/c positive cells (Fig. 3a, b).

The numbers of iNOS-positive cells as well as iNOS and CD11 b/c colocalized cells, in the peri-infarct area of mice in the M-high group were significantly suppressed compared to mice in the M-vehi group ($P < .01$). However, no significant difference was observed between the numbers of CD11b/c-positive immune cells in these two groups (Fig. 3c).

These results suggest that the number of immune cells, including macrophages and microglia, along with pro-inflammatory and neurotoxic phenotypes, are suppressed by the intravenous administration, of hAMSCs, although the total number of immune cells was not altered.

Blood Brain Barrier Permeability is Suppressed by the Administration of hAMSCs

In order to investigate the association between BBB permeability and neuro-inflammation, we performedan EB assay 24 h after administering the high dose of hAMSCs. BBB disruption was determined by the leakage of the EB stain (dark blue) into ipsilateral brain tissues (Fig. 4a). The EB levels in brain tissue were significantly decreased in the M-high group compared to those in the M-vehi group ($P < .05$) (Fig. 4b). This finding was also seen when the EB levels of ipsilateral brain tissues were corrected for those of contralateral side and brain dry weight ($P < .05$) (Fig. 4b). This result suggests that administration of hAMSCs protects the BBB from a potential breakdown due to ischemic infarction.

The Administration of hAMSCs Suppresses Delayed Neuronal Cell Death in the Peri-Infarct Area

Unlike necrosis at the ischemic core, which occurs within minutes following the onset of infarction, many neurons in the peri-infarct area undergo apoptosis after several hours or days following the onset of infarction. In fact, several reports have shown that neuronal death in the peri-infarct area and at the ischemic core are temporally and spatially different phenomena[36–38].

This prompted us to investigate the number of dying cells in the peri-infarct area at a relatively late phase of MCAO, namely 7 days following MCAO induction, using mice that were administered a high dose of hAMSCs on the day following MCAO.
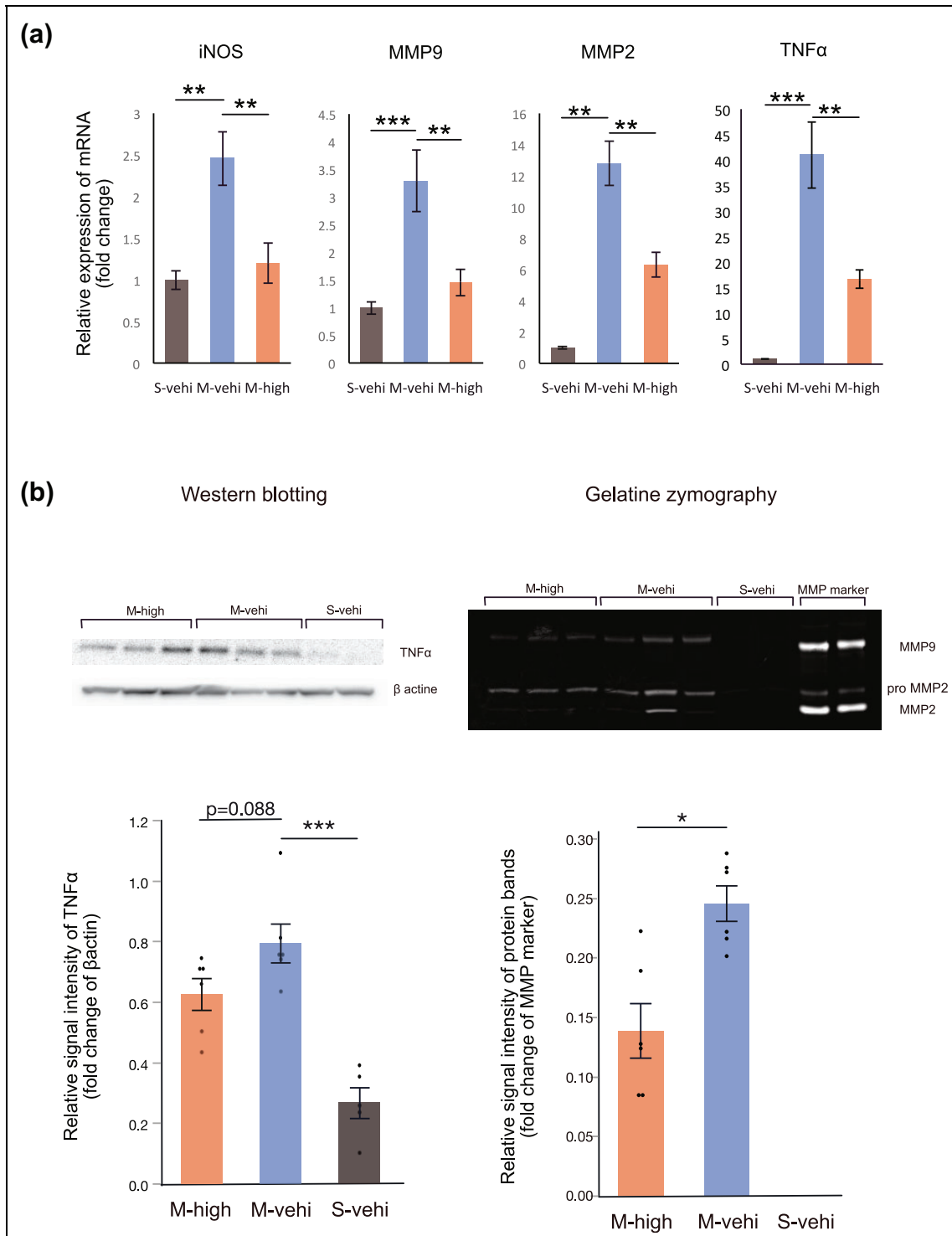
Figure 2. Administration of hAMSCs suppresses pro-inflammatory cytokines produced by immune cells following MCAO. We randomly assigned MCAO mice ($n = 12$) to one group administered a high-dose of hAMSCs (M-high: $n = 6$) and one group administered the vehicle control (M-vehi: $n = 6$). The hAMSCs were administered 24 h following MCAO induction and brain lysates were obtained 7 days following MCAO. Sham-operated mice (S-vehi; $n = 5$) were also examined. (a) Relative mRNA expression levels of inflammatory mediators compared to the endogenous NADPH control were evaluated via real-time qPCR. *$P < .05$, **$P < .01$, ***$P < .001$, for post-hoc Dunnett's test. (b, c) Representative gel images of western blots for TNFα and the gelatinase activity of MMP9 (M-high: $n = 6$; M-vehi: $n = 6$; S-vehi: $n = 5$). *$P < .05$, ***$P < .001$, post-hoc Dunnett's test and unpaired t test, respectively. For comparisons among more than three groups, one-way ANOVA was conducted first.
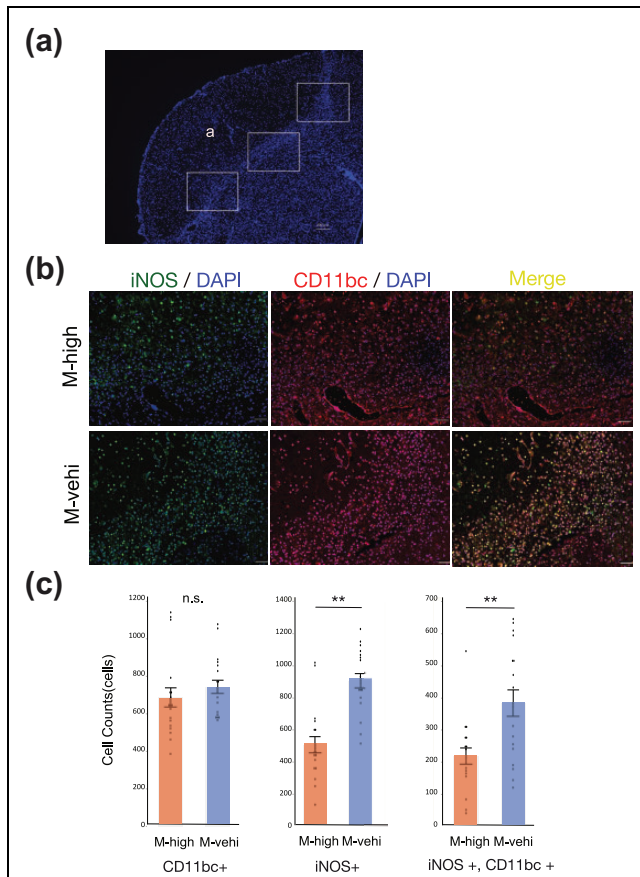
Figure 3. The administration of hAMSCs suppresses pro-inflammatory immune cells around the peri-infarct area. (a) Tissue section stained with 4′,6-diamino-2-phenylindole (DAPI) showing regions of analysis in the peri-infarct area ((a) ischemic core). Three random regions, indicated by solid boxes (200× magnification), per coronal section and two coronal sections per brain were analyzed to count iNOS+/CD11bc+ cells [M-high: $n = 3$; M-vehi: $n = 3$]. Scale bar: 200 μm. (b) Representative images of the immunofluorescent staining of brain sections in the M-high and M-vehi mice. iNOS (green) was colocalized (yellow) with CD11b/c (red). Nuclei were counterstained using DAPI (blue). Scale bar: 50 μm. 200× magnification. (c) Cell count of iNOS positive, CD11b/c positive, and iNOS/CD11bc colocalized cells. Scale bar: 50 μm. **$P < .01$, ***$P < .001$, unpaired *t*-test.

While disappearance of neuronal cells and cellular debris without nuclei were mainly observed in the ischemic core, TUNEL staining revealed that the number of TUNEL-positive neurons in the peri-infarcted area was significantly lower in the M-high group compared to the in M-vehi group ($P < .001$) (Fig. 5a, b). Moreover, western blotting of brain lysates extracted from the M-high mice 7 days following the MCAO operation, indicated a trend toward the suppression of the levels of the caspase 3 p17 subunit compared with M-vehi mice, although the difference was not statistically significant ($P = .1269$) (Fig. 5c).

These results suggest that the administration of hAMSCs suppresses delayed neuronal death in the peri-infarct area, particularly in relation with apoptosis.
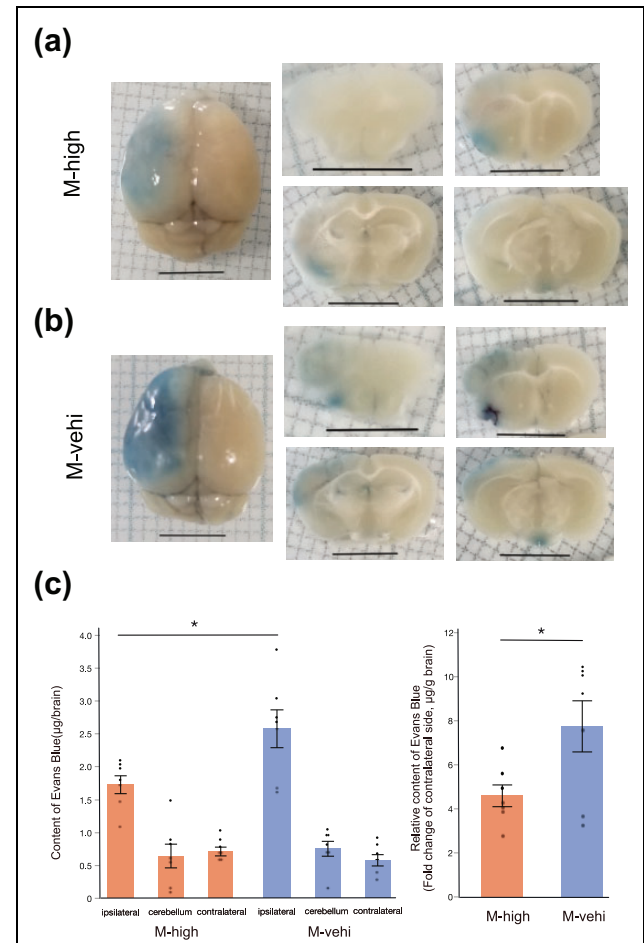

Figure 4. Evans Blue assay demonstrates the suppression of BBB permeability by the administration of hAMSCs. (a) Representative images of whole brain (left column) and coronal sections (middle and right columns). EB deposited in the brain parenchyma of the ischemic core and the peri-infarct area (middle cerebral artery territory of the left hemisphere), where the BBB was disrupted. Scale bar: 5 mm. (b) Quantitative analysis of EB content [M-high: $n = 8$; M-vehi: $n = 8$]. *; $P < .01$, unpaired *t*-test.

Discussion

Standard reperfusion therapies, such as the use of recombinant tissue plasminogen activator and endovascular thrombectomy, have very narrow therapeutic time windows. Because neuro-inflammation is considered to play an important role in the pathophysiology of ischemic stroke, immunosuppressive treatments that target single molecular pathways that are activated during the acute and subacute phases of ischemic infarction have been attempted, but have failed to demonstrate sufficient effects[11,12]. This may partly be due to post-ischemic inflammation, which acts through multiple pathways, and also plays an important role in tissue repair, and so immunosuppressive treatments that inhibit inflammation could interfere with these repair processes[2].

Cell therapy also targets the subacute phases of ischemic stroke, thereby preventing early secondary cell death by
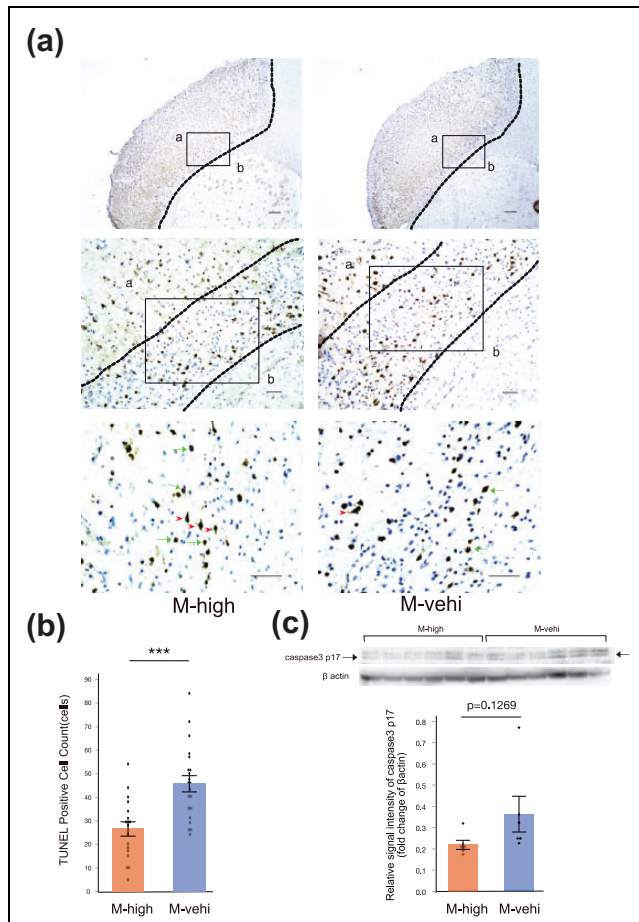
Figure 5. Administration of hAMSCs suppresses delayed neuronal apoptosis in the peri-infarct area. (a) Representative image of terminal deoxynucleotidyl transferase (TdT)-mediated dUTP nick end labelling (TUNEL) staining. Regions of analysis in the peri-infarct area are indicated by solid boxes (a: ischemic core, b: normal brain). Three random regions, indicated by solid boxes (400× magnification), per coronal section and two coronal sections per brain were analyzed to estimate the number of TUNEL positive cells [M-high: $n = 3$; M-vehi: $n = 3$]. Apoptotic nuclei (green arrows) showed peripheral chromatin clumping, blebbing, and fragmentation, whereas the cytoplasm of necrotic cells was homogeneously labeled (red arrowheads). Upper row: 4× magnification, Scale bar: 200 μm; middle row: 20× magnification, Scale bar: 50 μm; bottom row: 40× magnification, Scale bar: 50 μm. (b) Cell count of apoptotic cells in the peri-infarct area. ***$P < .001$, unpaired *t*-test. (c) Representative image of a western blot for caspase 3 p17 subunit.

suppressing apoptosis and inflammation[14]. Cell therapy has the potential to suppress multiple injury mechanisms and facilitate the mechanisms of cerebral repairment and reorganization during the subacute and chronic phases via angiogenesis, neurogenesis, and synaptogenesis[14,21].

Among the various transplantable cells, amniotic stem cells exhibit several features that make them an ideal donor source for cell therapy purposes[19]. Firstly, these cells are easily and less invasively obtained from amniotic membranes, which are usually discarded after birth, compared

to bone-marrow derived and adipose derived MSCs. Secondly, unlike the uses of ES cells, there are no ethical barriers to the use of amniotic stem cells. Thirdly, they have low immunogenicity resulting in a lack of host response following xenotransplantation, thereby enhancing the suitability of these cells for allogeneic therapeutic application. Finally, there is no evidence of tumorigenicity following the transplantation of isolated human amniotic cells into animal models[19,21].

The current study demonstrated that the expression levels of major pro-inflammatory cytokines, such as TNFα, iNOS, MMP2, and MMP9, were significantly decreased by the administration of hAMSCs to a mouse model of MCAO. These findings are substantiated by previous studies which have shown the expression levels of pro-inflammatory cytokines are suppressed by cell therapies[39,40].

We analyzed MMP gelatinase activities in the MCAO mice and showed that the MMP9 activity was decreased by hAMSC administration whereas MMP2 gelatinase activity was unchanged. This may be partly due to MMP2 being associated with the reversible disruption of the BBB during the early phases of infarction, in contrast to MMP9, which is elevated in the late phase resulting in the loss of tight junctions and is therefore considered to be principally responsible for disruption of the BBB[41,42]. These findings are compatible with the results of our evaluation of BBB integrity via EB extravasation[43].

We also demonstrated that the number of CD11b/c and iNOS double positive immune cells infiltrating the peri-infarct area, 7 days following MCAO, was significantly decreased by the hAMSC administration although there was no obvious difference in the number of CD11 b/c positive immune cells between the group administered hAMSCs and the vehicle control group.

CD11b is a phenotypic marker of macrophages, such as monocyte derived infiltrating macrophages and microglias (yolk-sac derived resident brain parenchymal macrophages), as well as meningeal and perivascular macrophages[44]. CD11c is expressed on granulocytes and dendritic cells as well as on macrophages[45]. However, iNOS is expressed in macrophages, neutrophils, and microglia in response to pro-inflammatory cytokines, and generates excessive NO, leading to the production of peroxynitrite, which exhibits neurotoxic action[46]. Its expression level is generally used to distinguish M1 pro-inflammatory macrophages/microglia from M2 anti-inflammatory macrophages/microglia[47-49].

Macrophages and microglia are known to have a spectrum of different but overlapping functional phenotypes, namely the M1 and M2 phenotypes[6]. Similar phenotypic differentiation is also observed in dendritic cells[50]. M1 macrophages typically release tissue-damaging pro-inflammatory mediators whereas M2 macrophages work as scavengers of cellular debris and produces various protective/trophic factors. A unique chronological phenotype shift from M2-dominant to M1-dominant is caused by the M2-to-M1 conversion within activated microglia/macrophages and

the continuing recruitment of pro-inflammatory M1 microglia/macrophages following ischemic infarction[49]. Amnion derived stem cells reportedly limit M1 polarization and promote M2 polarization[51]. These results substantiate our findings showing that although the number of M1 phenotypic iNOS-positive immune cells was reduced by hAMSC administration, the total amount of immune cells including M2 phenotypic immune cells was not altered, suggesting that hAMSC administration suppresses the M2-to-M1 phenotypic shift during the subacute phase. This finding was also compatible with the results of a previous study of ours which investigated the effect of adipose-derived mesenchymal stem cells (ADSCs) on ischemic stroke, where the total CD11b+ cell counts in the subacute phase were not very different, but the M1 phenotype immune cells were found to be significantly higher in the vehicle control than in the group administered ADSCs[52].

Finally, we evaluated the effect of hAMSCs on apoptosis in the peri-infarct areas. Despite differences in the routes used for administration (i.e., intracerebral, intravenous) and the time points of assessment (from 24 h to 21 d after transient MCAO), several studies have indicated that neuronal apoptosis around the ischemic infarction is suppressed by the administration of amniotic stem cells[39,43,53–55]. Although TUNEL staining is not always a specific indicator of apoptosis[32], when combined with typical changes in nuclear morphology, it can be utilized to distinguish the apoptotic cells from the necrotic ones. Our data on the peri-infarct areas, 7 days after MCAO, showed suppression of delayed cell death, with particular reference to apoptotic neuronal death, by hAMSCs, which substantiates previous findings. Western blotting of the caspase 3 p17 subunit also suggested that the administration of hAMSCs has a suppressive effect on activated apoptotic pathways, although this effect was not statistically significant. This may be because apoptotic neuronal death only accounts for a portion of total cell death, since necrotic and apoptotic cell deaths occur concomitantly in ischemic lesions, where the dominant cell death process depends on the relative speed of each process[33]. Apoptotic cell death in the peri-infarct areas appears to occur during the later phases, compared to necrosis in the ischemic core, which may enable the hAMSCs to extend the therapeutic window and be effective, even after the failure of reperfusion therapy for ischemic stroke.

Taken together, our findings indicate that suppression of pro-inflammatory cytokines and the M2-to-M1 phenotype shift, by administering hAMSCs intravenously, appears to inhibit BBB breakdown and apoptosis in the peri-infarct areas, resulting, in turn, in an improvement of neurological outcomes.

Compared to intravenous administration, the clinical use of intracranial injections has some limitations. Intracranial injection, which requires suitable imaging facilities and surgical expertise, may cause adverse effects such as periprocedural hemorrhage, surgical site infection, and brain damage leading to further BBB breakdown and inflammatory responses[21].

Moreover, most importantly, this approach does not target the systemic immune response that contributes to impaired outcomes following ischemic infarction[51].

The relatively small diameter of amniotic stem cells (8–15 μm) probably reduces the likelihood of these cells clumping inside lung capillaries, and indeed, it has been suggested that amnion derived stem cells acutely administered intravenously to mice following the onset of cerebral ischemia underwent a significant migration to the spleen as well as the injured brain via stromal cell derived factor 1(SDF1)-CXCR4 signaling[54,56,57]. Additionally, in several reports, splenectomy before the induction of stroke has shown to reduce infarct size, as well as the number of activated mononuclear immune cells in the ischemic hemisphere, and to diminish the efficacy of intravenously administered amnion derived stem cells[54,58].

Although there are challenges in differentiating monocyte-derived macrophages from resident brain parenchymal microglia and their relative degree of involvement in the M2-M1 phenotype shift in the brain, using a bone marrow chimeric technique in models of experimental autoimmune encephalomyelitis (EAE), Ajami et al. showed that significant monocyte recruitment into the brain was found only in animals that already displayed considerable disease activity and that progression to severe EAE was strongly correlated with the extent of this myelomonocytic infiltration[59]. Additionally M2 microglia (i.e. resident brain parenchymal macrophages) have been reported to show a greater tendency to maintain their M2 status than monocyte derived M2 macrophage in vitro[60]. Taken together, the spleen appears to play an important role in the acute influx of M1 phenotypic immune cells into the brain after stroke, which is at least partly the underlying mechanism of the M2-M1 phenotype shift in the brain that leads to disruption of the BBB, and might be a target for intravenously administered hAMSCs[61], although it cannot be denied that hAMSCs directly suppress intraparenchymal inflammation in the brain and disruption of BBB leading to a reduction in acute M1 myelomonocytic infiltration. This emphasizes the importance of evaluating the efficacy of administering hAMSCs intravenously.

As confirmed by other studies[39,54], we demonstrated that the subacute intravenous administration of hAMSCs (a day after MCAO induction), ameliorated long-term neurological deficits in a mouse model following cerebral infarction. Furthermore, for the first time we report that the effect of amnion derived mesenchymal stem cells is dose dependent. These findings could distinguish the cell therapy by intravenous administration of hAMSCs from conventional reperfusion therapies in the clinical setting, when considering that it could still be effective in the acute phase even after the failure of hyperacute conventional reperfusion therapies via definitely different mechanisms by suppressing apoptosis as well as neuroinflammation.

However, several previous studies have suggested that the delayed administration of hAMSCs after the stroke-induced

brain injury has already established itself (1–3 d following the onset of stroke) may still effectively enhance long-term functional recovery[54]. This recovery seems to be partly due to the promotion of M2 macrophage polarization by the amnion derived stem cells[51], further resulting in the release of anti-inflammatory cytokines (IL-10, IL-6) and growth factors, including angiogenic factors[20], which assist in the brain repair process[62]. Moreover, it has been suggested that amnion derived stem cells may differentiate toward a neural lineage in vivo[21]. The current study is beset with certain limitations. One such limitation is that we did not assess whether the brain parenchyma or spleen was more important in terms of the target point for intravenously administered hAMSCs, even though we demonstrated the possibility that a certain number of stem101-positive hAMSCs migrated into the brain parenchyma. Another limitation is that the effects of hAMSCs on the anti-inflammatory, neuro-protective, and neuro-regenerative processes in the subacute and chronic phases were not evaluated.

In regard to future studies, it may be helpful to investigate the mechanisms underlying the differentiation of hAMSCs into a neuronal lineage, which strongly supports the need to administer the hAMSCs themselves, instead of conditioned medium obtained from hAMSCs.

Conclusion

In conclusion, the current study demonstrates that administering hAMSCs improves neurological deficits in a mouse model of ischemic stroke. The underlying mechanisms of such improvements appears to be the suppression of pro-inflammatory cytokines and the shift from a M2 to a M1 phenotype, resulting in a reduction in the breakdown of the BBB and reduced apoptosis in peri-infarct areas. The effects of administering hAMSCs on delayed and chronic phases, including anti-inflammatory, neuro-protective, and neuro-regenerative effects, warrant further investigation.

Availability of data and materials

The authors confirm that all data underlying the findings are fully available without restriction. The datasets used and/or analyzed during the current study are available from the corresponding author on reasonable request.

Authors Contribution

YY conducted experiments, analyzed the data, and drafted the manuscript. TT participated in experimental design and the manuscript revision. YK, KT and MS participated in experimental design, data analysis and interpretation, and manuscript preparation. KY isolated, expanded, and formulated the hAMSCs as an investigational drug. ND made substantial contributions to the analysis of behavioral tasks. SY made substantial contributions to the study conception and design, approved the final version of the article to be published, and agreed to be accountable for all aspects of the work. All authors have read and approved the final manuscript.

ORCID iD

Yoji Kuramoto https://orcid.org/0000-0002-3652-6261
Shinichi Yoshimura https://orcid.org/0000-0001-5633-9132

Reference

1. Katan M, Luft A. Global burden of stroke. Semin Neurol. 2018;38(2):208–211.
2. Iadecola C, Anrather J. The immunology of stroke: from mechanisms to translation. Nat Med. 2011;17(7):796–808.
3. Carden DL, Granger DN. Pathophysiology of ischaemia-reperfusion injury. J Pathol. 2000;190(3):255–266.
4. Peerschke EI, Yin W, Ghebrehiwet B. Complement activation on platelets: implications for vascular inflammation and thrombosis. Mol Immunol. 2010;47(13):2170–2175.
5. Eltzschig HK, Carmeliet P. Hypoxia and inflammation. N Engl J Med. 2011;364(7):656–665.
6. Benakis C, Garcia-Bonilla L, Iadecola C, Anrather J. The role of microglia and myeloid immune cells in acute cerebral ischemia. Front Cell Neurosci. 2014;8:461.

7. Shichita T, Sakaguchi R, Suzuki M, Yoshimura A. Post-ischemic inflammation in the brain. Front Immunol. 2012;3: 132.

8. Konsman JP, Drukarch B, Van Dam AM. (Peri)vascular production and action of pro-inflammatory cytokines in brain pathology. Clin Sci (Lond). 2007;112(1):1–25.

9. Engelhardt B, Sorokin L. The blood-brain and the blood-cerebrospinal fluid barriers: function and dysfunction. Semin Immunopathol. 2009;31(4):497–511.

10. Carvajal HG, Suarez-Meade P, Borlongan CV. Amnion-derived stem cell transplantation: a novel treatment for neurological disorders. Brain Circ. 2016;2(1):1–7.

11. Jin R, Liu L, Zhang S, Nanda A, Li G. Role of inflammation and its mediators in acute ischemic stroke. J Cardiovasc Transl Res. 2013;6(5):834–851.

12. Lakhan SE, Kirchgessner A, Hofer M. Inflammatory mechanisms in ischemic stroke: therapeutic approaches. J Transl Med. 2009;7:97.

13. Song CG, Zhang YZ, Wu HN, Cao XL, Guo CJ, Li YQ, Zheng MH, Han H. Stem cells: a promising candidate to treat neurological disorders. Neural Regen Res. 2018;13(7):1294–1304.

14. Stonesifer C, Corey S, Ghanekar S, Diamandis Z, Acosta SA, Borlongan CV. Stem cell therapy for abrogating stroke-induced neuroinflammation and relevant secondary cell death mechanisms. Prog Neurobiol. 2017;158:94–131.

15. Caplan AI, Dennis JE. Mesenchymal stem cells as trophic mediators. J Cell Biochem. 2006;98(5):1076–1084.

16. Lee HK, Finniss S, Cazacu S, Xiang C, Brodie C. Mesenchymal stem cells deliver exogenous miRNAs to neural cells and induce their differentiation and glutamate transporter expression. Stem Cells Dev. 2014;23(23):2851–2861.

17. Wang Y, Chen X, Cao W, Shi Y. Plasticity of mesenchymal stem cells in immunomodulation: pathological and therapeutic implications. Nat Immunol. 2014;15(11):1009–1016.

18. Hao L, Zou Z, Tian H, Zhang Y, Zhou H, Liu L. Stem cell-based therapies for ischemic stroke. Biomed Res Int. 2014; 2014:468748.

19. Yu SJ, Soncini M, Kaneko Y, Hess DC, Parolini O, Borlongan CV. Amnion: a potent graft source for cell therapy in stroke. Cell Transplant. 2009;18(2):111–118.

20. Manuelpillai U, Moodley Y, Borlongan CV, Parolini O. Amniotic membrane and amniotic cells: potential therapeutic tools to combat tissue inflammation and fibrosis? Placenta. 2011;32(Suppl 4):S320–S325.

21. Broughton BR, Lim R, Arumugam TV, Drummond GR, Wallace EM, Sobey CG. Post-stroke inflammation and the potential efficacy of novel stem cell therapies: focus on amnion epithelial cells. Front Cell Neurosci. 2012;6:66.

22. Yamahara K, Harada K, Ohshima M, Ishikane S, Ohnishi S, Tsuda H, Otani K, Taguchi A, Soma T, Ogawa H, Katsuragi S, et al. Comparison of angiogenic, cytoprotective, and immunosuppressive properties of human amnion- and chorion-derived mesenchymal stem cells. PLoS One. 2014;9(2):e88319.

23. Tsuda H, Yamahara K, Otani K, Okumi M, Yazawa K, Kaimori JY, Taguchi A, Kangawa K, Ikeda T, Takahara S, Isaka Y. Transplantation of allogenic fetal membrane-derived mesenchymal stem cells protects against ischemia/reperfusion-induced acute kidney injury. Cell Transplant. 2014;23(7):889–899.

24. Ohshima M, Yamahara K, Ishikane S, Harada K, Tsuda H, Otani K, Taguchi A, Miyazato M, Katsuragi S, Yoshimatsu J, Kodama M, et al. Systemic transplantation of allogenic fetal membrane-derived mesenchymal stem cells suppresses Th1 and Th17 T cell responses in experimental autoimmune myocarditis. J Mol Cell Cardiol. 2012;53(3): 420–428.

25. Otagiri S, Ohnishi S, Miura A, Hayashi H, Kumagai I, Ito YM, Katsurada T, Nakamura S, Okamoto R, Yamahara K, Cho KY, et al. Evaluation of amnion-derived mesenchymal stem cells for treatment-resistant moderate Crohn's disease: study protocol for a phase I/II, dual-centre, open-label, uncontrolled, dose-response trial. BMJ Open Gastroenterol. 2018;5(1):e000206.

26. Yamahara K, Hamada A, Soma T, Okamoto R, Okada M, Yoshihara S, Yoshihara K, Ikegame K, Tamaki H, Kaida K, Inoue T, et al. Safety and efficacy of amnion-derived mesenchymal stem cells (AM01) in patients with steroid-refractory acute graft-versus-host disease after allogeneic haematopoietic stem cell transplantation: a study protocol for a phase I/II Japanese trial. BMJ Open. 2019;9(7):e026403.

27. Taguchi A, Kasahara Y, Nakagomi T, Stern DM, Fukunaga M, Ishikawa M, Matsuyama T. A Reproducible and Simple Model of Permanent Cerebral Ischemia in CB-17 and SCID Mice. J Exp Stroke Transl Med. 2010;3(1):28–33.

28. Winter B, Juckel G, Viktorov I, Katchanov J, Gietz A, Sohr R, Balkaya M, Hortnagl H, Endres M. Anxious and hyperactive phenotype following brief ischemic episodes in mice. Biol Psychiatry. 2005;57(10):1166–1175.

29. Kilic E, Kilic U, Bacigaluppi M, Guo Z, Abdallah NB, Wolfer DP, Reiter RJ, Hermann DM, Bassetti CL. Delayed melatonin administration promotes neuronal survival, neurogenesis and motor recovery, and attenuates hyperactivity and anxiety after mild focal cerebral ischemia in mice. J Pineal Res. 2008;45(2): 142–148.

30. Kadam SD, Mulholland JD, Smith DR, Johnston MV, Comi AM. Chronic brain injury and behavioral impairments in a mouse model of term neonatal strokes. Behav Brain Res. 2009;197(1):77–83.

31. Sun MK, Alkon DL. Open space swimming test to index anti-depressant activity. J Neurosci Methods. 2003;126(1):35–40.

32. Charriaut-Marlangue C, Margaill I, Represa A, Popovici T, Plotkine M, Ben-Ari Y. Apoptosis and necrosis after reversible focal ischemia: an in situ DNA fragmentation analysis. J Cereb Blood Flow Metab. 1996;16(2):186–194.

33. Unal-Cevik I, Kilinc M, Can A, Gursoy-Ozdemir Y, Dalkara T. Apoptotic and necrotic death mechanisms are concomitantly activated in the same cell after cerebral ischemia. Stroke. 2004; 35(9):2189–2194.

34. Imai T, Takagi T, Kitashoji A, Yamauchi K, Shimazawa M, Hara H. Nrf2 activator ameliorates hemorrhagic transformation in focal cerebral ischemia under warfarin anticoagulation. Neurobiol Dis. 2016;89:136–146.

35. D'Hooge R, De Deyn PP. Applications of the Morris water maze in the study of learning and memory. Brain Res Brain Res Rev. 2001;36(1):60–90.

36. Broughton BR, Reutens DC, Sobey CG. Apoptotic mechanisms after cerebral ischemia. Stroke. 2009;40(5):e331–e339.

37. Nicotera P, Lipton SA. Excitotoxins in neuronal apoptosis and necrosis. J Cereb Blood Flow Metab. 1999;19(6):583–591.

38. Sairanen T, Karjalainen-Lindsberg ML, Paetau A, Ijas P, Lindsberg PJ. Apoptosis dominant in the periinfarct area of human ischaemic stroke–a possible target of antiapoptotic treatments. Brain. 2006;129(Pt 1):189–199.

39. Tao J, Ji F, Liu B, Wang F, Dong F, Zhu Y. Improvement of deficits by transplantation of lentiviral vector-modified human amniotic mesenchymal cells after cerebral ischemia in rats. Brain Res. 2012;1448:1–10.

40. Cheng Z, Wang L, Qu M, Liang H, Li W, Li Y, Deng L, Zhang Z, Yang GY. Mesenchymal stem cells attenuate blood-brain barrier leakage after cerebral ischemia in mice. J Neuroinflammation. 2018;15(1):135.

41. Yang Y, Estrada EY, Thompson JF, Liu W, Rosenberg GA. Matrix metalloproteinase-mediated disruption of tight junction proteins in cerebral vessels is reversed by synthetic matrix metalloproteinase inhibitor in focal ischemia in rat. J Cereb Blood Flow Metab. 2007;27(4):697–709.

42. Dejonckheere E, Vandenbroucke RE, Libert C. Matrix metalloproteinases as drug targets in ischemia/reperfusion injury. Drug Discov Today. 2011;16(17-18):762–778.

43. Faezi M, Nasseri Maleki S, Aboutaleb N, Nikougoftar M. The membrane mesenchymal stem cell derived conditioned medium exerts neuroprotection against focal cerebral ischemia by targeting apoptosis. J Chem Neuroanat. 2018;94:21–31.

44. Li Q, Barres BA. Microglia and macrophages in brain homeostasis and disease. Nat Rev Immunol. 2018;18(4):225–242.

45. Posel C, Uri A, Schulz I, Boltze J, Weise G, Wagner DC. Flow cytometric characterization of brain dendritic cell subsets after murine stroke. Exp Transl Stroke Med. 2014;6(1):11.

46. Garry PS, Ezra M, Rowland MJ, Westbrook J, Pattinson KT. The role of the nitric oxide pathway in brain injury and its treatment–from bench to bedside. Exp Neurol. 2015;263:235–243.

47. Liu C, Li Y, Yu J, Feng L, Hou S, Liu Y, Guo M, Xie Y, Meng J, Zhang H, Xiao B, et al. Targeting the shift from M1 to M2 macrophages in experimental autoimmune encephalomyelitis mice treated with fasudil. PLoS One. 2013;8(2):e54841.

48. Michelucci A, Heurtaux T, Grandbarbe L, Morga E, Heuschling P. Characterization of the microglial phenotype under specific pro-inflammatory and anti-inflammatory conditions: Effects of oligomeric and fibrillar amyloid-beta. J Neuroimmunol. 2009;210(1-2):3–12.

49. Hu X, Leak RK, Shi Y, Suenaga J, Gao Y, Zheng P, Chen J. Microglial and macrophage polarization-new prospects for brain repair. Nat Rev Neurol. 2015;11(1):56–64.

50. Ludewig P, Gallizioli M, Urra X, Behr S, Brait VH, Gelderblom M, Magnus T, Planas AM. Dendritic cells in brain diseases. Biochim Biophys Acta. 2016;1862(3):352–367.

51. Evans MA, Broughton BRS, Drummond GR, Ma H, Phan TG, Wallace EM, Lim R, Sobey CG. Amnion epithelial cells - a novel therapy for ischemic stroke? Neural Regen Res. 2018; 13(8):1346–1349.

52. Tatebayashi K, Takagi T, Fujita M, Doe N, Nakagomi T, Matsuyama T, Yoshimura S. Adipose-derived stem cell therapy inhibits the deterioration of cerebral infarction by altering macrophage kinetics. Brain Res. 2019;1712:139–150.

53. Aboutaleb N, Faezi M, Nasseri Maleki S, Nazarinia D, Razavi Tousi SMT, Hashemirad N. Conditioned medium obtained from mesenchymal stem cells attenuates focal cerebral ischemia reperfusion injury through activation of ERK1/ERK2-BDNF signaling pathway. J Chem Neuroanat. 2019;97:87–98.

54. Evans MA, Lim R, Kim HA, Chu HX, Gardiner-Mann CV, Taylor KWE, Chan CT, Brait VH, Lee S, Dinh QN, Vinh A, et al. Acute or delayed systemic administration of human amnion epithelial cells improves outcomes in experimental stroke. Stroke. 2018;49(3):700–709.

55. Nazarinia D, Aboutaleb N, Gholamzadeh R, Nasseri Maleki S, Mokhtari B, Nikougoftar M. Conditioned medium obtained from human amniotic mesenchymal stem cells attenuates focal cerebral ischemia/reperfusion injury in rats by targeting mTOR pathway. J Chem Neuroanat. 2019;102:101707.

56. Robin AM, Zhang ZG, Wang L, Zhang RL, Katakowski M, Zhang L, Wang Y, Zhang C, Chopp M. Stromal cell-derived factor 1alpha mediates neural progenitor cell motility after focal cerebral ischemia. J Cereb Blood Flow Metab. 2006; 26(1):125–134.

57. Wang Y, Deng Y, Zhou GQ. SDF-1alpha/CXCR4-mediated migration of systemically transplanted bone marrow stromal cells towards ischemic brain lesion in a rat model. Brain Res. 2008;1195:104–112.

58. Ajmo CT Jr., Vernon DO, Collier L, Hall AA, Garbuzova-Davis S, Willing A, Pennypacker KR. The spleen contributes to stroke-induced neurodegeneration. J Neurosci Res. 2008; 86(10):2227–2234.

59. Ajami B, Bennett JL, Krieger C, McNagny KM, Rossi FM. Infiltrating monocytes trigger EAE progression, but do not contribute to the resident microglia pool. Nat Neurosci. 2011;14(9):1142–1149.

60. Girard S, Brough D, Lopez-Castejon G, Giles J, Rothwell NJ, Allan SM. Microglia and macrophages differentially modulate cell death after brain injury caused by oxygen-glucose deprivation in organotypic brain slices. Glia. 2013;61(5):813–824.

61. Shiao ML, Yuan C, Crane AT, Voth JP, Juliano M, Stone LLH, Nan Z, Zhang Y, Kuzmin-Nichols N, Sanberg PR, Grande AW, et al. Immunomodulation with human umbilical cord blood stem cells ameliorates ischemic brain injury - a brain transcriptome profiling analysis. Cell Transplant. 2019;28(7):864–873.

62. Anrather J, Iadecola C. Inflammation and stroke: an overview. Neurotherapeutics. 2016;13(4):661–670.